CHAPTER 1

BACKGROUND AND LITERATURE REVIEW: THE USE OF UNMANNED AERIAL VEHICLES FOR AEROBIOLOGICAL SAMPLING

INTRODUCTION

Agricultural biota (e.g., seeds, insects, pollen, plant pathogens, etc.) may be transported over long distances in the atmosphere. It is important to understand the methods and techniques of airborne transport so as to minimize the propagation of unwanted species in crops that are important for human welfare. The long distance transport of biota takes place primarily in the planetary boundary layer (PBL) of the atmosphere—the layer of the atmosphere extending from approximately 50 m to 1 km above the surface of the earth. Investigators have identified and characterized seeds (Shields et. al. 2006), insects (Shields et al., 1999), and fungi in the PBL. One of the attractive techniques for characterizing specific airborne species is to collect samples at different altitudes under a variety of environmental conditions (e.g., day/night, temperature, humidity, and wind conditions). One method that enables aerobiological sampling at various altitudes is the use of remotely controlled aircraft designed to fly specific patterns and collect aerobiological samples at an altitude of interest. Remotely piloted vehicles (RPV) have been used for aerobiological sampling in agricultural ecosystems. This prior work, which is summarized briefly later in this chapter, provides a foundation and motivation for the current work. Agents that cause plant disease are thought to travel long distances in the atmosphere and the transport mechanisms are not well understood.

STUDY OF THE POTATO LEAFHOPPER IN THE LOWER ATMOSPHERE

Remotely piloted vehicles (RPVs) have been used in the past to collect insects from the lower atmosphere (Shields et al., 1999). The insect of interest was the potato leafhopper, *Empoasca fabae* (Homoptera: Cicadellidae), which is a pest to many crops. This insect is believed to travel long distances during migrating seasons in the PBL aided by wind to get from one field to another. This is related to the work that we have done since they used an RPV with a device that could be opened to sample at a desired altitude.

The RPV used for this study was the Senior Telemaster, which has a 2.4 m wingspan and was powered by a 24 cc gasoline engine. The RPVs were outfitted with nets mounted to the top of the wing surface to collect the potato leafhopper. The net was closed during takeoff and landing and opened after reaching the desired altitude for collection. To safely control the RPV, two RC receivers were installed so the RPV could be landed under reduced control in the event of an RC link failure. In this setup, one receiver controlled one side of the RPV (right aileron, right elevator) while the other receiver controlled the other side of the RPV (left aileron, left elevator). Throttle was controlled by one receiver and the rudder was controlled by the other receiver. The RPV was equipped with sensors for measuring altitude, airspeed, and GPS position and this data was transmitted to the ground where it could be monitored with a laptop computer. The person monitoring the data could then give feedback to the pilot to better control the RPV.

STUDY OF HORSEWEED IN THE PLANETARY BOUNDARY LAYER

Horseweed (*Conyza Canadensis*) is an agricultural weed that can reduce crop yield by as much as 90%. Recently, horseweed has developed resistance to herbicides. Resistant horseweed has the potential to spread through the atmosphere over long distances, and colonize agricultural fields in new geographic locations. Shields et. al. (2006) used RPVs to study the long distance transport of horseweed. They used an RPV monoplane with a 3-m wingspan powered by a 50 cc gasoline two-stroke engine. The RPV was designed specifically for use in agricultural sampling on undeveloped runways. The RPV was flown at full throttle at a speed of 26 m/s (96 km/h) at an altitude of 30 meters. The seed collectors were mounted under each wing near the wing tips to minimize the effects of the turbulent air from the propeller disturbing the sampled air. The sampling devices were constructed using sail servos intended for small RC boats. Each RPV carried two collectors that were capable of collecting two samples each, for a total of four samples per flight. A standard 90-mm petri plate was modified by cutting the bottom of the plate off and affixing a cloth mesh with 30-μm openings to the bottom of the plate. The trapping surface was sprayed with a sticky adhesive just before the flight to retain any seeds that struck the surface. The RPV used an onboard microcomputer to record and transmit telemetry data which included altitude, airspeed, and GPS position. This data was used to aid in controlling the aircrafts altitude by relay the information from a person watching a computer to the pilot. A total of 17 flights were conducted over a three day period in September 1998 in which 36 intact seeds were collected.

STUDY OF THE ABUNDACE OF THE FUNGAL PLANT PATHOGEN **GIBBERELLA ZEAE** *IN THE PLANETARY BOUNDARY LAYER*

The most relevant research related to this work is the collection of *Gibberella zeae* in the planetary boundary layer using RPVs (Maldonado-Ramirez et al., 2005). The RPV used for this collection had a 2.4 m wingspan and used four spore-sampling devices. The spore-sampling devices were made using sail RC servos intended to lift the sail on an RC boat. They were used for their high torque capabilities. The servos had 90 mm diameter petri plates attached to the end of wooden arms extending from the servo. The plates would be closed during takeoff and landing to avoid contamination of the plates from biota that was not at the desired altitude. Once the desired altitude was reached, the collection plates would be opened by a RC switch from the ground. Each sampling plate was exposed to approximately 8 m^3 of air per minute with the RPV cruising at 20 m/s. The sampling flights would last 15 minutes, exposing the media to approximately 120 m^3 of air. A total of 12,858 viable spores of *Gibberella zeae* were collected during 158 flights over four consecutive years. The RPV was equipped with sensors for measuring altitude, airspeed, and GPS position and this data was transmitted to the ground where it could be monitored with a laptop computer. This data was transmitted to the ground where it could be monitored with a laptop computer and then relayed to the pilot to better control the RPV.

STUDY OF THE USE OF AUTONOMOUS SYSTEMS IN AGRICULTURE

A wide variety of autonomous systems has been applied to agricultural applications. They include air vehicles used to spray agricultural fields with fungicides or herbicides,

to sample airborne contaminates, and to take photographs of agricultural fields. Autonomous ground vehicles have been developed to harvest and to perform soil preparation and sampling.

MicroPilot, one of the leading autopilot manufacturers in the world, developed a UAV to monitor agricultural fields. A small hand-launched UAV was equipped with a stripped down Pentax digital camera and called the system "CropCam." The CropCam system allowed farmers to monitor their own fields instead of hiring expensive professional aerial photographers. The system would fly over the field and take GPS stamped digital images before returning home. The system has an estimated cost of $7,000 (Flight Global, 2006).

Autonomous systems for agricultural applications have not been limited to aerial vehicles. Investigators at Virginia Tech have designed an autonomous broccoli inspection and harvesting robot (Ramirez, 2006). The work focused on the development of software and a computer vision system to locate the heads of broccoli using Hough transforms of the lines on the stems and leaves. A co-occurrence matrix analysis produced the location of the head and a statistical texture analysis was performed to determine the maturity of the broccoli head. The work also included recommendations on the type of vehicles that could be used to incorporate the developed software to autonomously harvest the broccoli (Ramirez, 2006).

CHAPTER 2

DESIGN OF AN AUTONOMOUS UNMANNED AERIAL VEHICLE FOR AEROBIOLOGICAL SAMPLING

INTRODUCTION

Previous studies have relied on radio controlled (RC) Unmanned Aerial Vehicles (UAVs) also called RPVs to collect meaningful data in the atmosphere (Maldonado-Ramirez, 2005). There are some unavoidable problems with using RC for this purpose that include poor positional accuracy, poor altitude accuracy, and pilot fatigue. It is very difficult for any RC pilot to maintain a precise flight path at the same altitude for a given amount of time, which leads to high variability in the flight path. The use of an autonomous UAV can address nearly all the problems associated with RPVs. As part of the present study, we designed autonomous unmanned aerial vehicle (UAV) systems to improve the positional accuracy, altitude accuracy, and to reduce pilot fatigue when used for aerobiological sampling.

PLATFORM FOR AN AUTONOMOUS UAV

The Senior Telemaster Almost Ready to Fly (STARF) (Hobby Lobby International, Inc., Brentwood, TN) was used as our aerial sampling platform. The STARF has a wingspan of 94" with 1330 in^2 of wing area and 320 in^2 of rear stabilizer area. The stock STARF construction plans suggest a 0.61 in^3 engine. We used an O.S. 1.20 in^3 engine (O.S. Engines, Champaign, IL) that produces 3.1 hp at 9,000 rpm (**Figure 2.1**). A Master Airscrew 15x8 inch K-Series propeller (Windsor Propeller Company, Rancho Cordova,

CA) was mounted to the engine. The larger engine was used to create more power to pull the sampling plates through the air (since the plates, when open, create a considerable amount of drag). The factory engine mounts required trimming to allow the slightly wider engine. The servo tray was also modified to accommodate the autonomous system. The stock servo tray, which houses the rudder, elevator, and throttle servos, was cut in half to allow additional space inside the fuselage. Half of the servo tray was used to mount the rudder and elevator servos (**Figure 2.2**). The throttle servo was mounted in the front of the plane just behind the firewall to allow a pushrod to pass from its original intended location. Custom servo mounts were glued in place and a micro servo (Futaba S3101, Futaba, Champaign, IL) was installed to operate the throttle (**Figure 2.3**). A micro servo was used here since there is limited space and there would be no heavy load on the throttle servo at any time. The second half of the servo tray was modified for use as a platform to mount batteries above the remaining half of the servo tray. This makes the batteries easily accessible (**Figure 2.4**).

Figure 2.1. Senior Telemaster ARF with oversized 1.20AX engine.

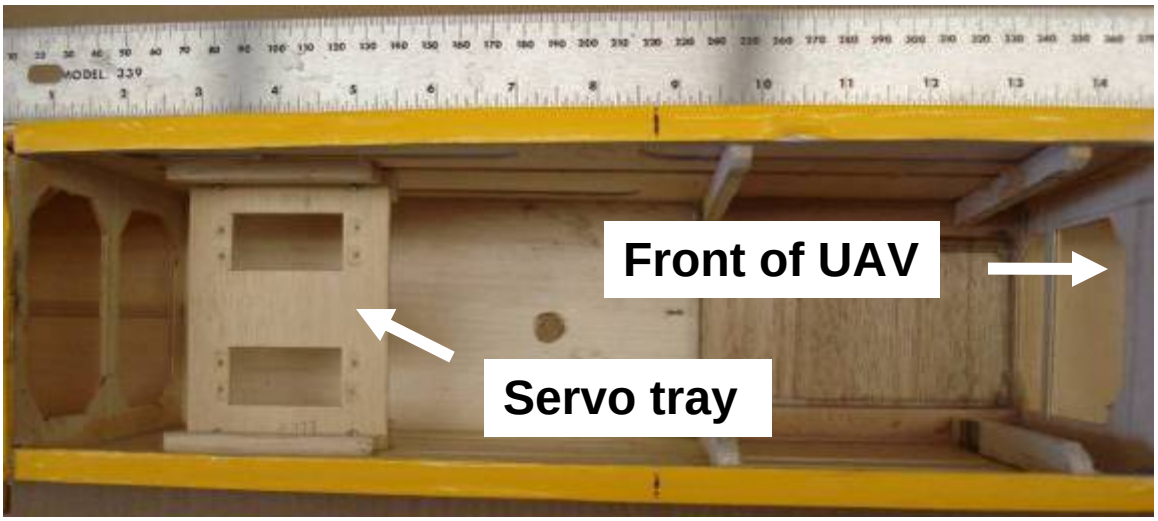

Figure 2.2. Top view showing how the servo tray was relocated to the back of the fuselage of the Senior Telemaster ARF.

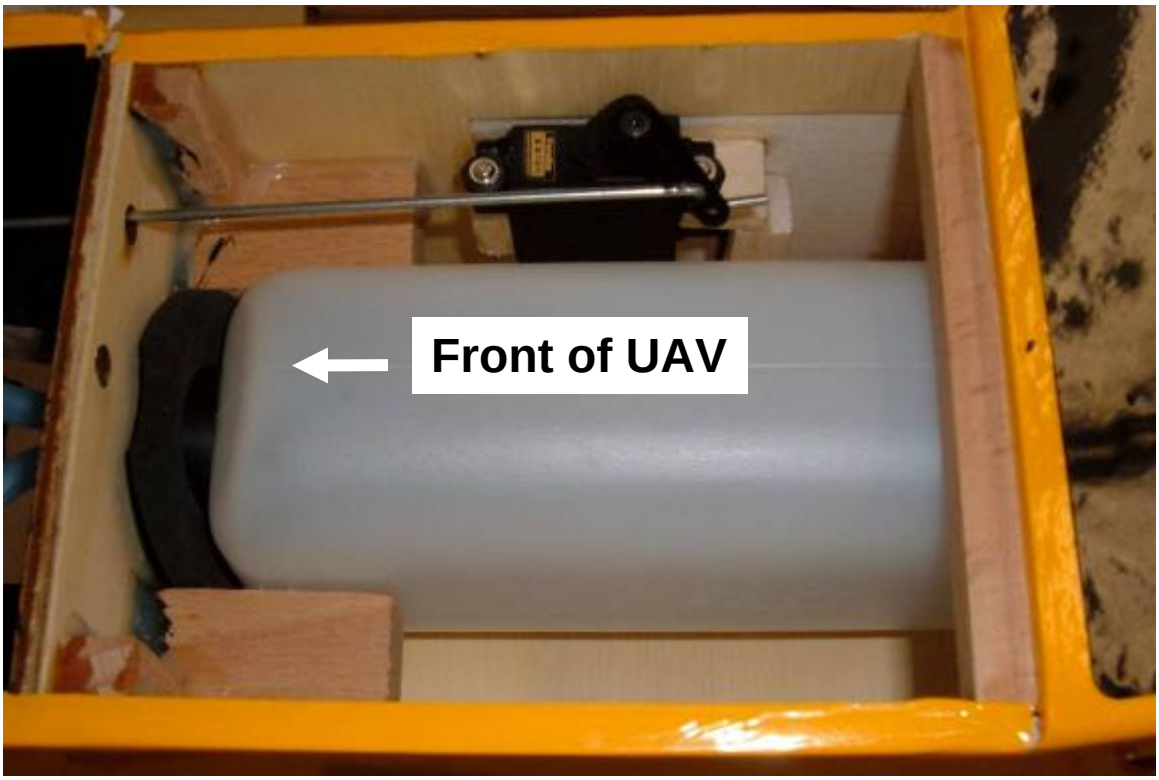

Figure 2.3. The throttle servo was relocated near the firewall on the Senior Telemaster ARF.

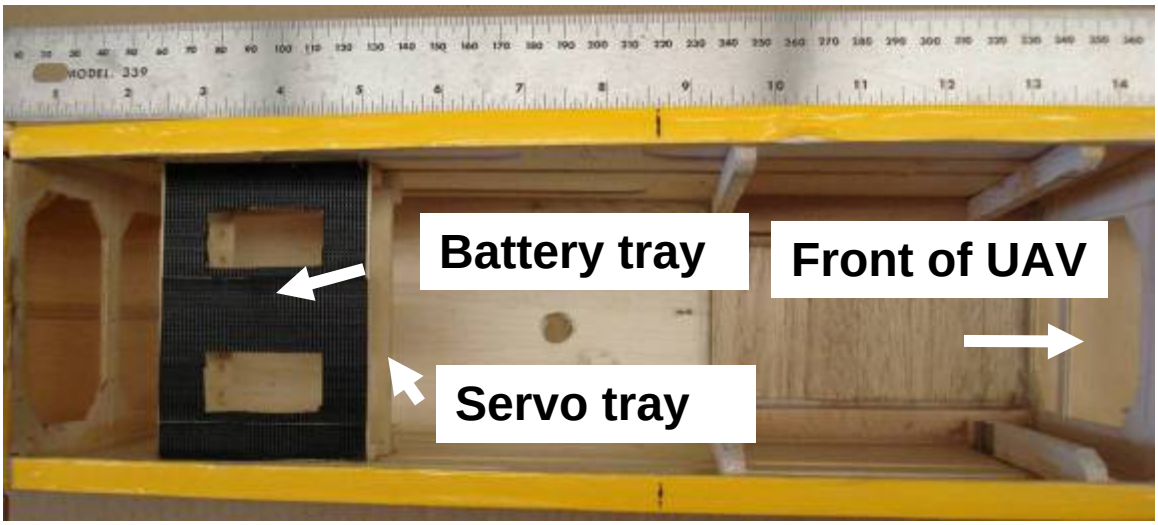

Figure 2.4. The battery tray was installed above servo the tray for accessibility.

The STARF kit included a pair of wing struts, but it did not include any hardware to install them. We used a removable clevis-hitch pin (881075/881096, Hillman, Cincinnati, OH) arrangement to install the wing struts (**Figure 2.5**). A custom ¾" aluminum bracket was constructed and mounted at the bottom of the fuselage. The clevis pins were glued into holes drilled into the bracket. The wing struts were mounted to the wings with standard control surface hinges (GPMQ3971, Great Planes, Champaign, IL), providing a secure joint between the strut and the wing. On the other end of the struts, a hole was drilled to accept the clevis. Washers were attached with epoxy around the holes to reinforce the connection.

Figure 2.5. Wing strut attachment method on the Senior Telemaster ARF.

AUTONOMOUS SYSTEM

Flight Controller. We used the MicroPilot MP2028^{g} system (MicroPilot Inc., Stony Mountain, Manitoba, Canada) as our autonomous flight controller. The MicroPilot MP2028^{g} system is lightweight (28 grams), has good functionality, and is relatively affordable. The system permits the plane to navigate GPS waypoints through a desired sampling area while providing the user with real-time dynamic control of flight characteristics. The autopilot system is a printed circuit board that is equipped with 3-axis gyros and accelerometers. These components provide inertial measurements to allow control of the roll, pitch, and yaw of the UAV. A GPS unit attached to the board receives satellite signals through the attached antenna. A static pressure sensor allows the autopilot to measure relative altitude. The autopilot can also use GPS-based altitude data to fly. Since this data is known to have a wide error band, it is not used for controlling flight. A pitot tube pressure sensor is used to track the airspeed of the UAV. This sensor

was extended with tubing away from the fuselage to the leading edge of the wing on the opposite side of the engine muffler to obtain accurate results.

A compass module (MP-COMP, MicroPilot Inc.) was added to the MicroPilot to allow it to determine the true heading of the UAV. This heading is used in addition to the GPS heading. This was particularly important for dealing with windy flying conditions. The combination of GPS heading, compass heading, GPS speed, and airspeed allowed the autopilot to calculate wind velocity and direction, ultimately resulting in more precise control of the flight path. An ultrasonic above ground level (AGL) sensor (MP-AGL, MicroPilot Inc.) was added to permit autonomous take-off and landing. This sensor uses an ultrasonic transducer mounted on the bottom side of the fuselage to accurately calculate distances to ground level at altitudes below five meters. The sensor is connected to the autopilot via a shielded coaxial cable. An analog to digital converter (ADC) (MP-ADC, MicroPilot Inc.) was added to allow for additional parameters to be monitored such as additional battery voltages that are used to power other components.

All of the control surfaces on the aircraft were controlled by the autopilot. The signal for the servos passed through a servo board, allowing the power supply to the servo to be independent of the power supply to the MicroPilot. The plane can be controlled manually via a 72MHz RC transmitter. The receiver (FUTJ7122, Futaba) on the UAV has its signal passed through the autopilot board. Control is transferred to and from the autopilot by a switch on the RC transmitter (FUTJ7122, Futaba). When in manual mode, the signal is simply passed through the autopilot to the servo board and the pilot on the ground had full control of all aspects of flight.

Control methods. MicroPilot used the Proportional, Integral, and Derivative (PID) control loop gains to monitor and control flight performance. The gains can be adjusted using ground control station software. The PID loops consisted of: (1) aileron from desired roll, (2) elevator from desired pitch, (3) rudder from Y-accelerometer, (4) rudder from heading, (5) throttle from speed, (6) throttle from glide slope, (7) pitch from altitude, (8) pitch from AGL altitude, (9) pitch from airspeed, (10) roll from heading, and (11) heading from cross track. All loops that control an actual control surface on the UAV is updated at a rate of 30 Hz which includes loops (1), (2), (3), and (4). All other control loops are updated at 5 Hz. The results from the inner loops (7, 8, 9, 10, and 11) are used as inputs to the outer control loops that control the actual control surfaces of the UAV. The gains were tuned to achieve the desired level of accuracy in flight (Dingus et al., 2006).

Ground control station. The ground control station (GCS) consisted of a laptop computer running MicroPilot Horizon (the ground control station software included with the purchase of MicroPilot). The UAV communicated with the GCS via a 900MHz radio modem, allowing real-time monitoring and control of nearly all aspects of flight. Flight files containing GPS waypoints can be modified and uploaded during flight. The Horizon software can be programmed to read any flight parameter or the output of the Analog to Digital Converter (ADC) and display the information on the laptop in real time. State values that were programmed to show on the graphical user interface (GUI) are altitude, airspeed, GPS speed, and compass heading (**Figure 2.6**).

Figure 2.6. Screen shot of MicroPilot Horizon GCS software.

Electronics box. An electronics project box was used to house all the MicroPilot components that needed to be installed in the UAV (**Figure 2.7**). This helped ensure that, in the event of damaging the UAV, the expensive electronics would not be easily damaged. A piece of plywood was cut to fit in the breadboard slots that are pre-formed around the inside of the box. This piece was used as the mounting surface for the autopilot board, compass, and ADC. The mounting orientation of the autopilot and the compass were critical to optimal control operation in the autopilot. The autopilot was mounted to the top of the plywood while the compass and the ADC were mounted to the bottom of the plywood. Slots were cut in the plywood to allow all necessary wiring to be connected between the components on opposite sides of the plywood. The servo board was mounted to the back side of the box to allow for easy connection of the servo wires without extra unnecessary wiring. Standard circuit board standoffs were glued to the box

to provide the desired spacing for the board. In order to do this, holes had to be cut into the back of the box for the mounting screws and the servo output terminals. The ultrasonic AGL was mounted in a similar fashion on the front of the box with its sensor connection exiting at the top front of the box. Mounting in this orientation allowed the sensor to be connected or disconnected without removal of the entire box. The lead for the GPS antenna was mounted in a hole drilled in the back of the box to allow for easy antenna removal. The required power was supplied through servo extensions passed through a rubber grommet installed in the back of the box. This method allows the use of standard RC power switches (SWH13, Futaba) to be mounted to the plane and then plugged directly into the extensions on the back of the electronics box. For the current design, four power switches were used: (1) autopilot, (2) radio modem, (3) servos, and (4) spore-samplers. The autopilot and the radio modem use separate 11.1 volt lithium-ion battery packs with 2200 mAh capacity (L18650-2200-3, Tenergy Corporation, Sunnyvale, CA). The UAV control surface servos used a 4.8 volt Nickel-Cadmium battery pack with 600 mAh capacity (NR-4J, Futaba) and the spore-samplers used a 4.8 volt Nickel Metal Hydride battery pack with 2000 mAh capacity (HCAM6320, Hobbico, Champaign, IL). Separate batteries were used for safety so that if one system was not working properly the other systems were not affected. This was done primarily because the large spore-sampler servos have the potential to draw very high amounts of power when they are opening and closing against the wind.

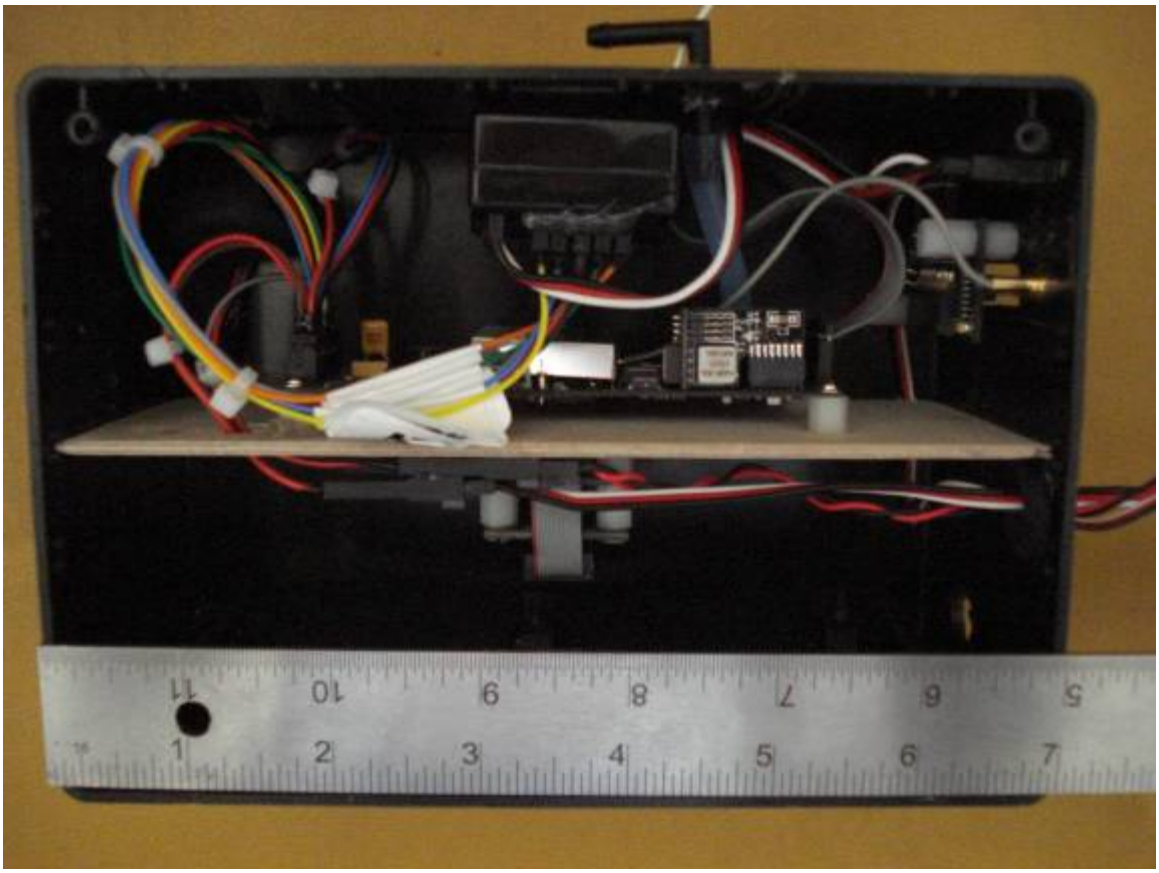

Figure 2.7. Electronics project box with components installed.

SPORE-SAMPLERS

The spore-sampling devices were designed with two large sail servos (HS-765HB, Hitec, Poway, CA) mounted in a wooden frame and attached to the bottom of the wing. The sail servos used are intended for use on an RC boat to lift the sails. Each servo controls an arm that has a Petri dish lid permanently attached to it. While sampling, a Petri dish bottom with the desired media is taped into the lid on the servo arm, allowing it to be opened and closed. Another lid is permanently attached to a piece of plywood mounted between the two servos. It extends forward to allow the Petri dishes on the arms to close into the lids on the plywood to avoid exposing the plates during take-off and landing.

In previous work by Maldonado-Ramirez et al. (2005) spore-sampling devices were mounted under the wing near the center of the wing chord and had servo arms that were approximately eight inches long (**Figure 2.8**). The major problem encountered with this design is the poor dynamic stability of the UAV when the sampling devices were opened or closed. When the sampling devices were opened to begin sampling, the plane would suddenly begin to pitch nose down since the devices introduced a large amount of drag below the aerodynamic center of the UAV. To remedy this problem, the sampling devices were redesigned to allow the Petri dishes to open on the leading edge of the wing (**Figure 2.9**). This change essentially eliminated the pitching of the UAV when the sampler devices were opened. The effective lifting force of the wing was reduced slightly, since there was now turbulent air flowing over the airfoil directly behind the sampling devices. On larger planes, this reduced lifting ability is typically not an issue since the UAV is not carrying its maximum payload.

Figure 2.8. Design of previous spore-sampling devices (Maldonado-Ramirez et al., 2005).

Figure 2.9. New and improved design of spore-samplers on the autonomous Senior Telemaster ARF. The spore-samplers open (bottom) and close (top) on the leading edge of the wing.

The sampling devices are not permanently mounted to the wings of the UAV. Rather, they are mounted using industrial strength Velcro to allow them to be removed when needed. This mounting method also allows the sampler to detach upon a very hard or crash landing, which helps to prevent the sampler from damaging the wing structure. Power and signal is provided to the sampler servos by 36 inch servo extensions (HCAM2726, Hobbico) routed inside the wing structure. Servo extensions were custom installed inside the wing with the plug flush with the bottom of the wing. The extensions were glued in place vertically to ensure that, if the sampling device was to become detached from the wing, then the servo wire would be pulled out by the weight of the sampler without ripping the extension through the structure of the wing. The four sampling servos were controlled via one RC channel that was routed through a servo synchronizer (MSA-10, Futaba) that allows the samplers to have an independent power

source from the rest of the UAV. Each servo can be adjusted independently to ensure the servo is moving in the correct direction and stopping at the appropriate places in both movement directions.

Two types of collection media have been used in our research: (1) *Fusarium*-selective medium that allows only *Fusarium* spp. to grow (**Figure 2.10**) and (2) potato dextrose agar which allows everything that is viable to grow (**Figure 2.11**).

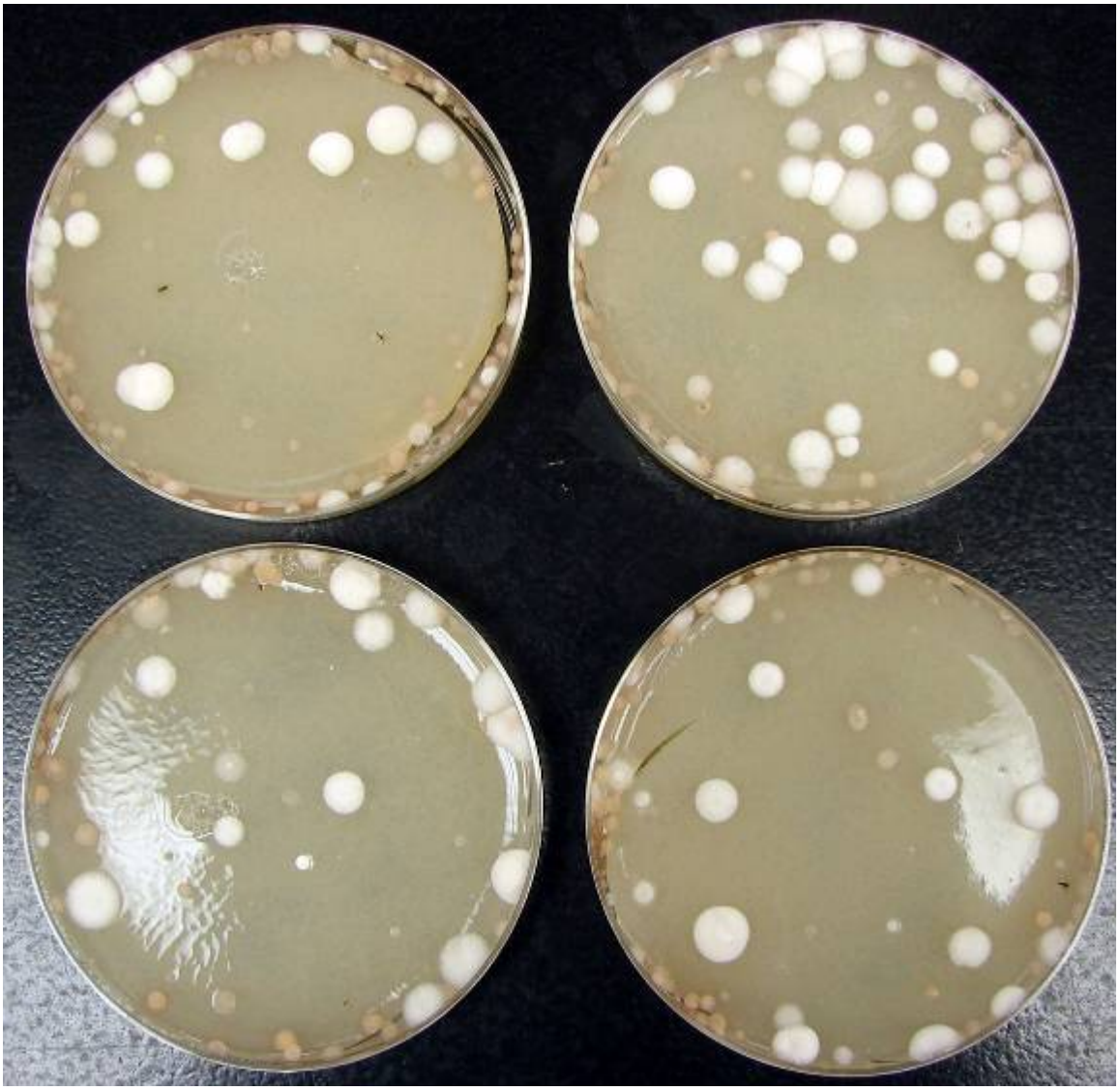

Figure 2.10. Plates of *Fusarium*-selective medium showing white *Fusarium* colonies collected 100 m above the surface of the earth at Virginia Tech's Kentland Farm.

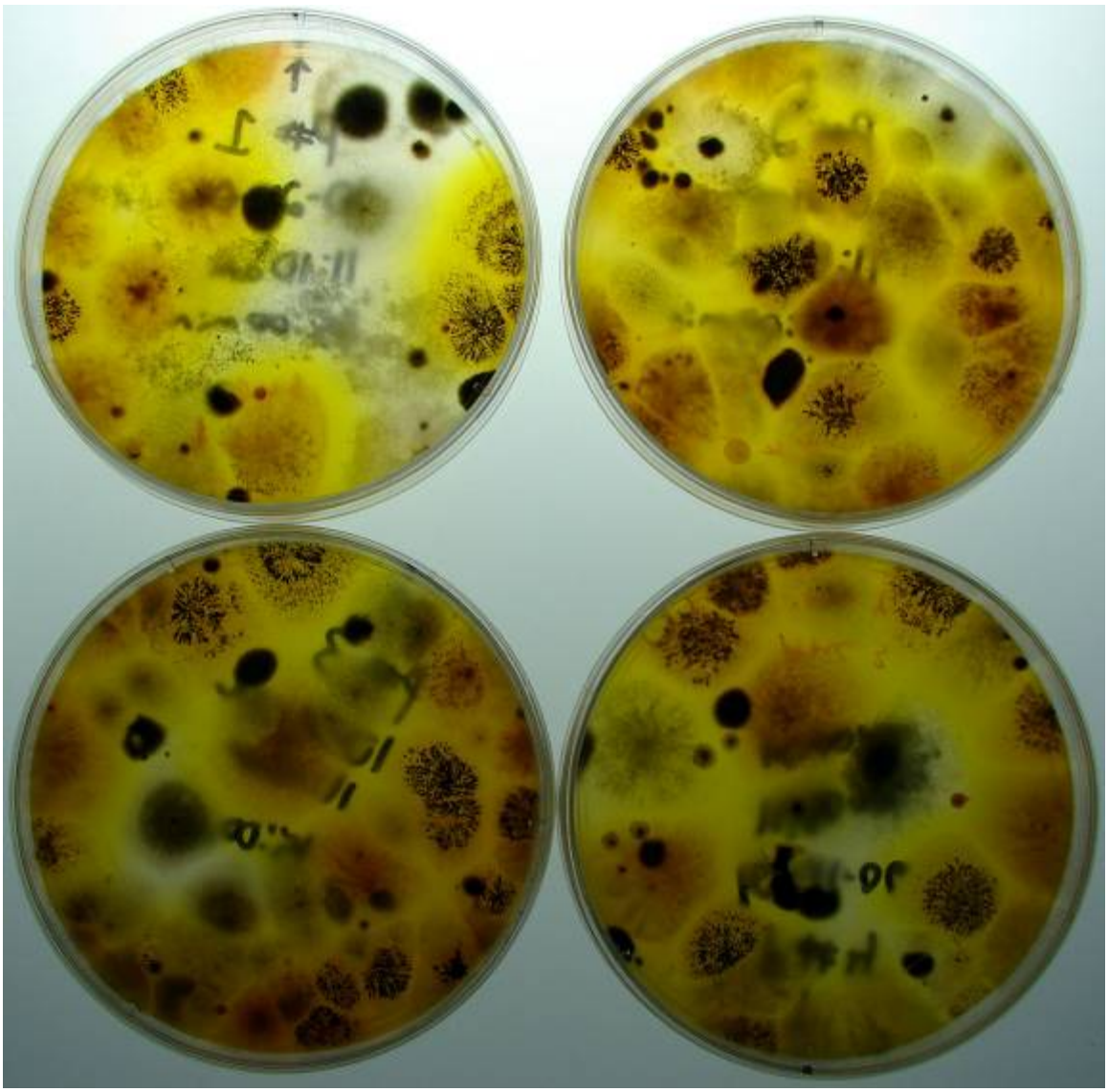

Figure 2.11. Culturable fraction of an atmospheric microbial community collected 100m above the surface of the earth at Virginia Tech's Kentland Farm. The plates contained a potato dextrose agar, a common medium for the cultivation of microbes.

CHAPTER 3

APPLICATION OF AN AUTONOMOUS UNMANNED AERIAL VEHICLE SYSTEM FOR CONSISTENT AEROBIOLOGICAL SAMPLING

INTRODUCTION

Autonomous UAVs have the potential to extend the range of aerobiological sampling, improve positional accuracy of sampling paths, and enable coordinated flight with multiple aircraft at different altitudes. To determine the most appropriate sampling path for aerobiological sampling, we explored a variety of different sampling patterns for our autonomous UAVs including multiple GPS waypoints plotted over a variety of spatial scales. It is important to define the parameters that may provide optimal performance of autonomous UAVs in a variety of different sampling environments. Position and altitude are two variables that are end results of the entire aircraft-building and gain-tuning process. We explored five different aerobiological sampling patterns that were defined by a series of GPS waypoints plotted over different spatial scales. The UAV was programmed to maintain a target altitude of 100m while flying the following five patterns: (1) single GPS waypoint, (2) two GPS waypoints, (3) three GPS waypoints, (4) four GPS waypoints, and (5) four GPS waypoints in a figure-8 pattern. The specific objectives of this study were to (1) determine the most appropriate sampling path for aerobiological sampling above agricultural fields, and (2) determine the most effective sampling pattern for maintaining a precise altitude during aerobiological sampling.

MATERIALS AND METHODS

Optimization of autonomous flight. The STARF was the UAV used to conduct aerobiological sampling experiments at Virginia Tech's Kentland Farm. We conducted a series of preliminary flights to adjust gains for the STARF. During these flights, we allowed the UAV to fly for 15 minutes under autopilot control without requiring RC manual override. We optimized our gains and achieved stable and consistent flight patterns with the sampling plates open since this would be when the UAV needed to perform best. Aerobiological data was collected during individual 15-minute sampling flights. We made small changes to the gains on the ground before each of the flight, flew for a 15-minute sampling flight, and tuned the gains appropriately on the ground before the next sampling flight. After 32 sampling flights, we arrived at an appropriate set of gains for the UAV. We used this set of optimized gains for the next 25 sampling flights; we did not make any further changes or adjustments to the autopilot during any of the remaining flights.

Data collection during flight. The full dataset from the autopilot containing all UAV states needed to conduct our analyses was downloaded directly from the autopilot after each flight. Data was imported into MATLAB for calculations and plotting. Maintaining an accurate altitude was considered to be the most important aspect of flight performance and aerobiological sampling, therefore most of the time tuning the gains was spent to reduce the variations in altitude during sampling. Also in this analysis the of the flight patterns, the positional consistency of the patterns was visually inspected within flights on a per loop basis and also compared between all different flights of the same pattern.

Autonomous patterns for aerobiological sampling. We chose five different GPS waypoint patterns based on the need for a UAV to be capable of sampling above most common size agricultural fields. These patterns were developed to keep the UAV within line of sight of the pilot, in the event that the pilot needed to take RC control of the aircraft during an emergency. The first pattern was a single GPS waypoint (**Figure 3.1**). Instead of progressing through the GPS waypoint, the autopilot positioned the UAV into a constant turn into the waypoint creating a circular pattern around the waypoint (**Figure 3.1**). The second pattern was two GPS waypoints separated by 325 meters (**Figure 3.2**). The UAV flew an elliptical path around the two points, successfully passing through each of the waypoints (**Figure 3.2**). The third pattern was three GPS waypoints arranged in an equilateral triangle with each leg measuring 325 meters (**Figure 3.3**). The UAV also successfully passed through each of the three waypoints (**Figure 3.3**). The fourth pattern was a four GPS waypoint rectangle measuring 325 meters by 150 meters (**Figure 3.4**). Due to the close proximity of the two waypoints separated by 150 meters, the autopilot usually navigated an oval around the outside of the rectangle passing through the waypoints at the end of the 325 meter leg (**Figure 3.4**). The fifth pattern was the same four GPS waypoints as the rectangle pattern, but the navigation order was changed to create a figure-8 sampling pattern (**Figure 3.5**). This pattern also utilized a different navigation command to navigate the longer legs of the pattern. The MicroPilot '*fromto*' command was used to force the autopilot to try to fly directly on the line connecting the waypoints instead of just flying towards the next waypoint. The effects of this command will be discussed in the results section.

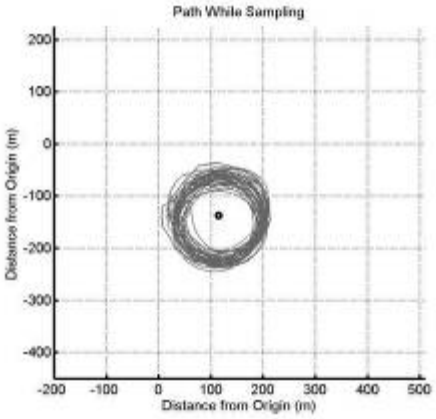

(A) Flight 34

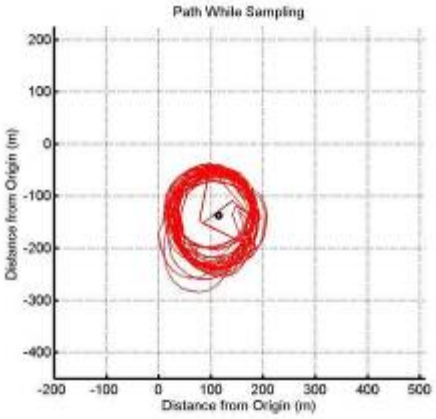

(B) Flight 35

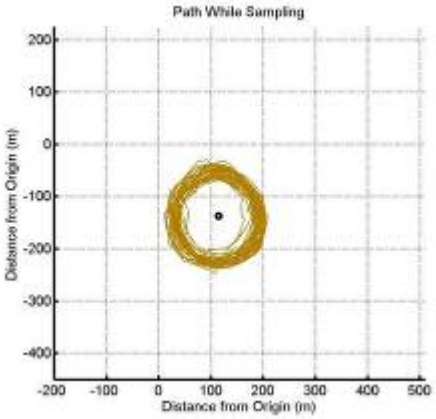

(C) Flight 40

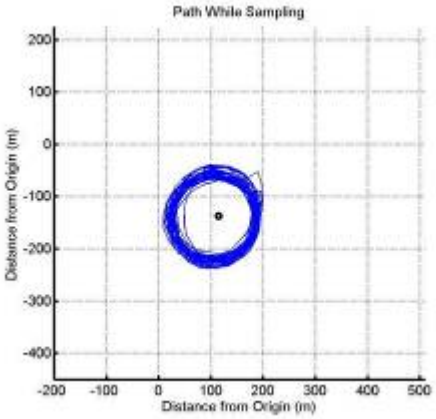

(D) Flight 41

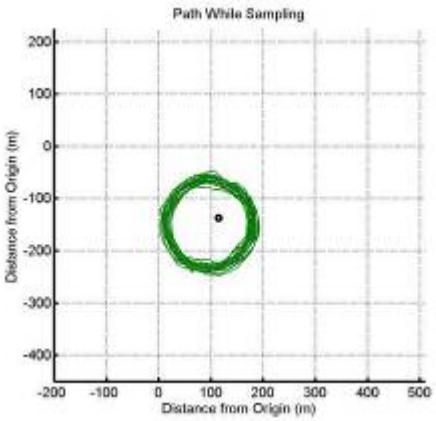

(E) Flight 42

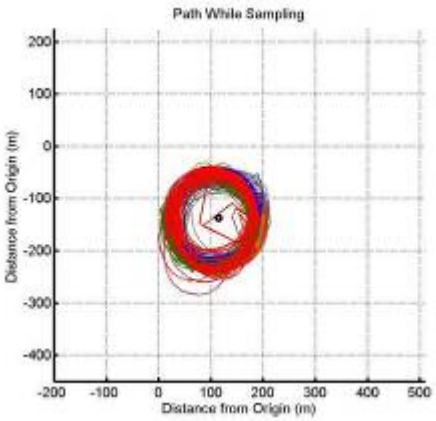

(F)

Figure 3.1. Autonomous flight patterns from for aerobiological sampling around a single GPS waypoint. Individual flight patterns (A-E), combined flight patterns (F).

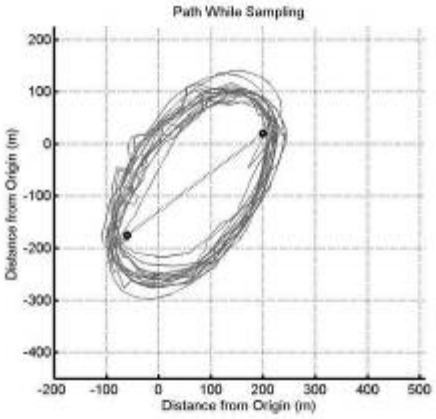

(A) Flight 43

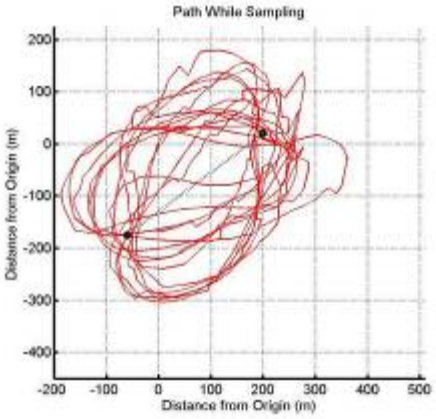

(B) Flight 48

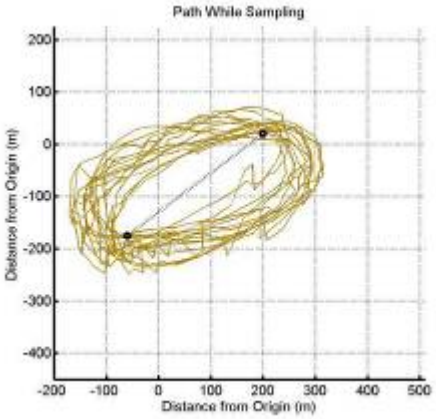

(C) Flight 50

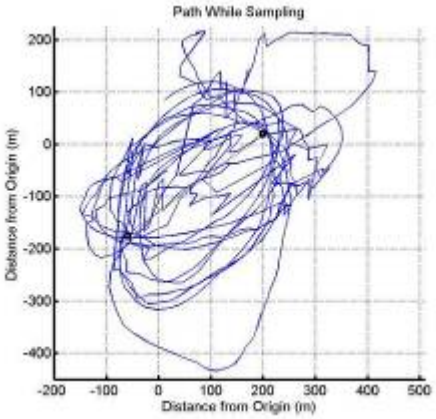

(D) Flight 51

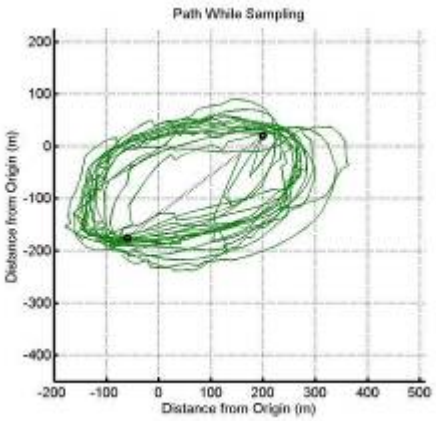

(E) Flight52

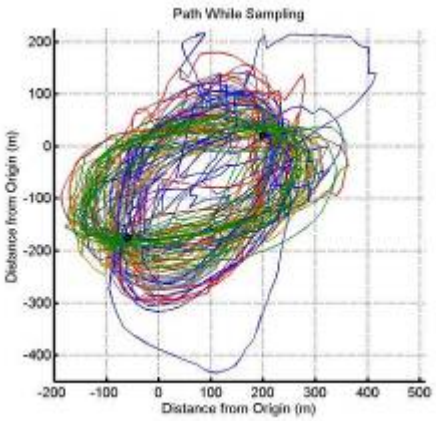

(F)

Figure 3.2. Autonomous flight patterns from for aerobiological sampling around two GPS waypoints. Individual flight patterns (A-E), combined flight patterns (F).

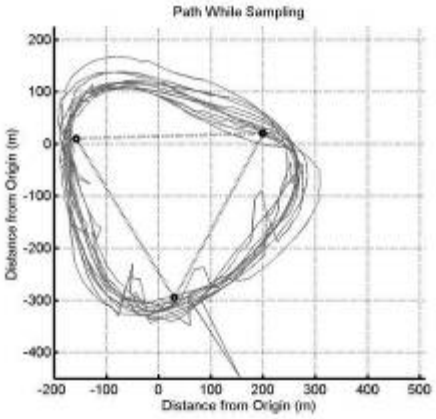

(A) Flight 37

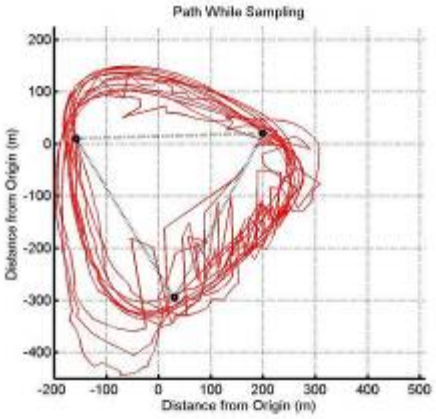

(B) Flight 38

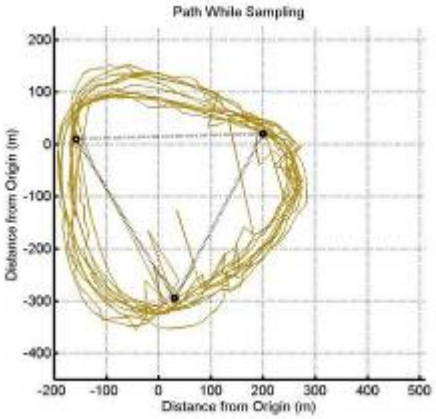

(C) Flight 39

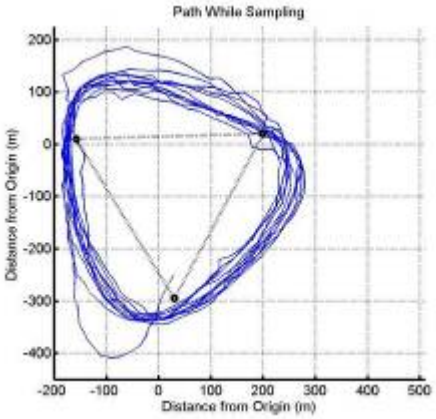

(D) Flight 58

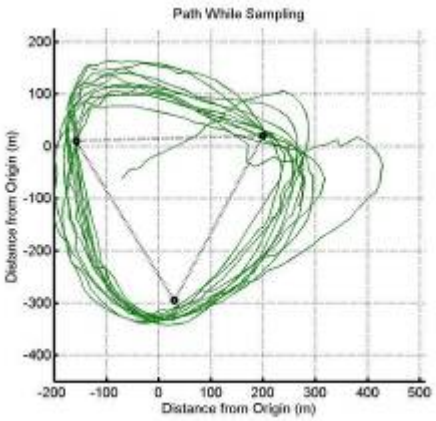

(E) Flight 59

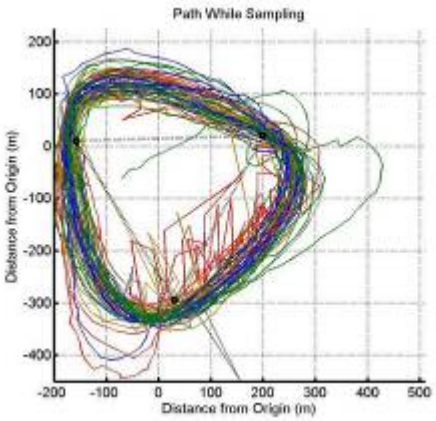

(F)

Figure 3.3. Autonomous flight patterns from for aerobiological sampling around three GPS waypoints. Individual flight patterns (A-E), combined flight patterns (F).

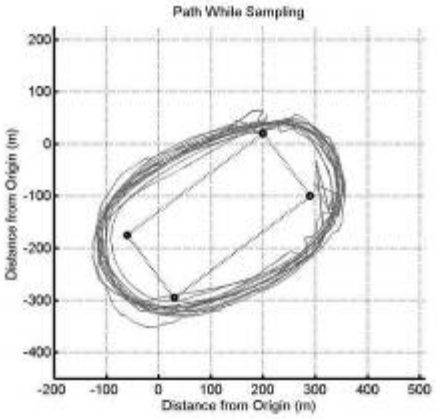

(A) Flight 36

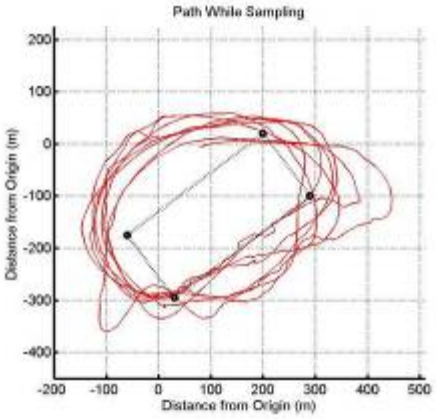

(B) Flight 44

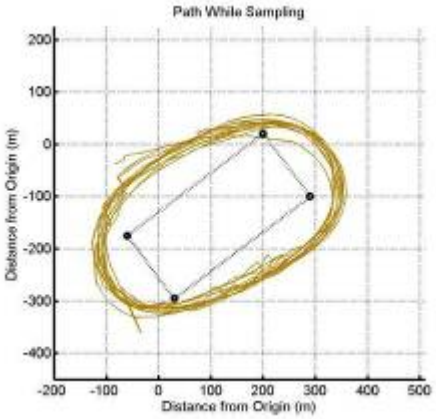

(C) Flight 46

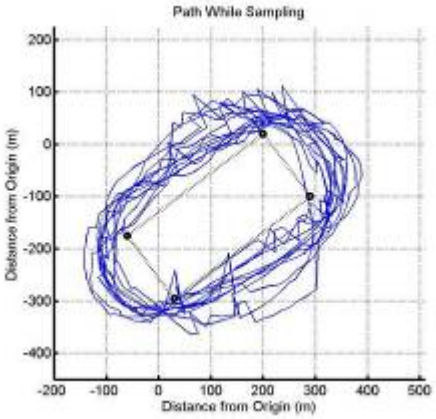

(D) Flight 49

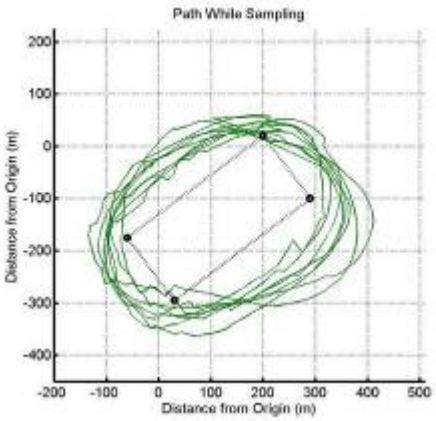

(E) Flight 53

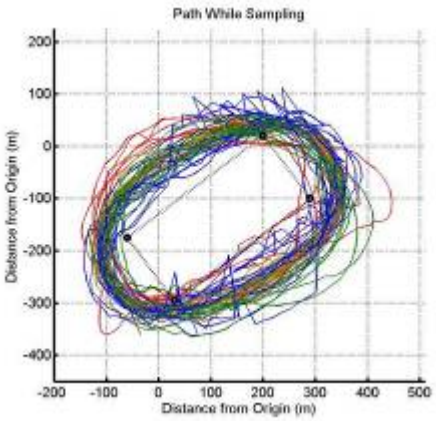

(F)

Figure 3.4. Autonomous flight patterns from for aerobiological sampling around four GPS waypoints. Individual flight patterns (A-E), combined flight patterns (F).

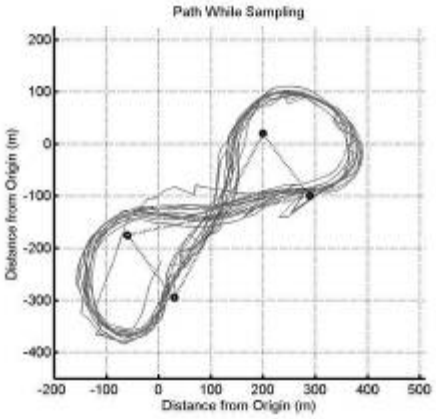

(A) Flight 33

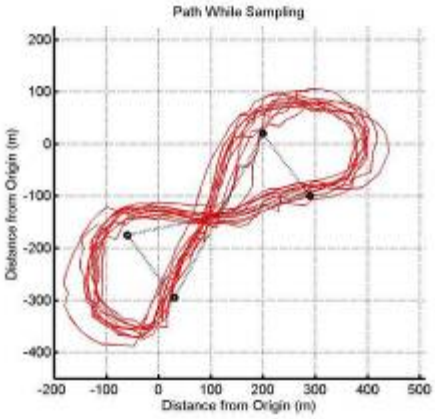

(B) Flight 54

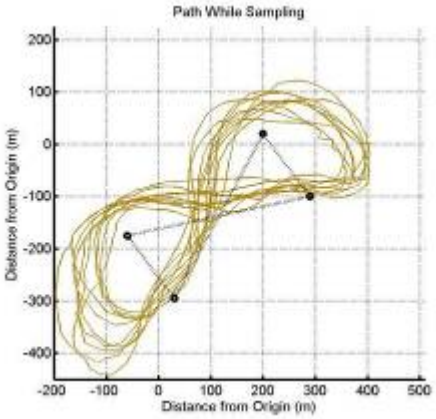

(C) Flight 55

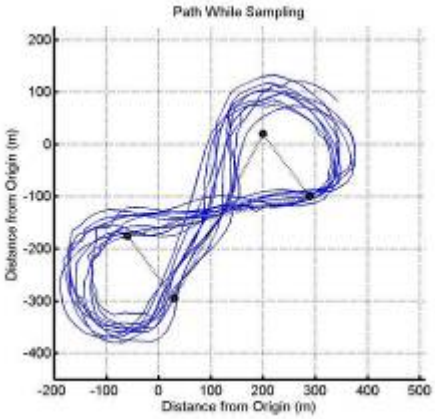

(D) Flight 56

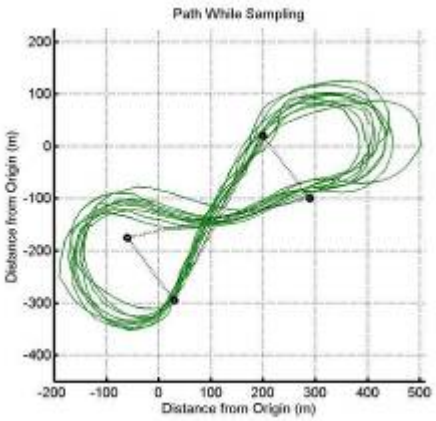

(E) Flight 57

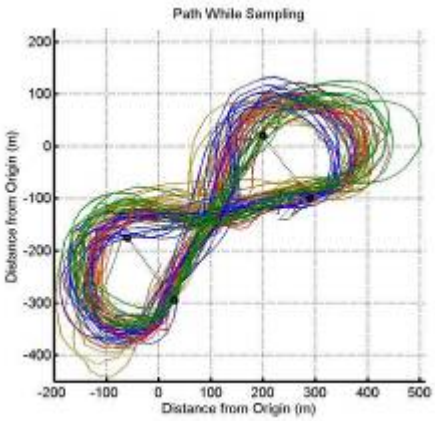

(F)

Figure 3.5. Autonomous flight patterns from for aerobiological sampling around four GPS waypoints in a figure-eight pattern. Individual flight patterns (A-E), combined flight patterns (F).

Comparison to remote-controlled flight. As a baseline for comparison, a flight was conducted when only RC control was used. The autopilot was used to collect sensor data rather than as flight controller. The single GPS waypoint pattern was flown. Based on the collected data, that point appeared to give the most accurate pattern. The manually piloted flight (**Figure 3.6**) was appears to be far less consistent than the autonomous flights with respect to altitude hold and positional accuracy.

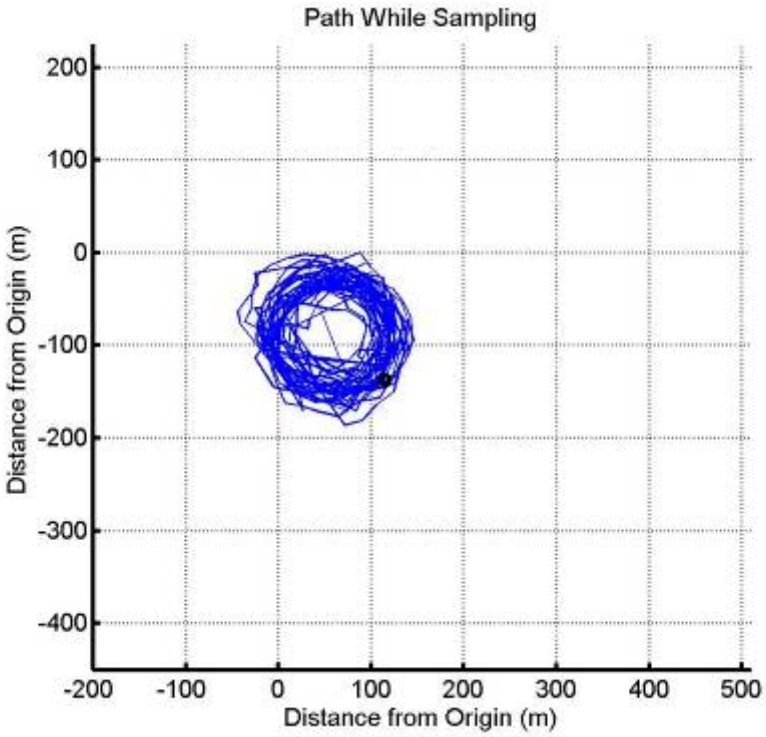

Figure 3.6. Inconsistent flight pattern from a remote-controlled aerobiological sampling flight around a single GPS waypoint.

RESULTS/DISCUSSION

We conducted a total of 25 autonomous aerobiological sampling flights for five different aerobiological sampling patterns. **Table 3.1** contains flight data for each of these 25 flights. The table contains the flight day and time, media type, aerobiological data,

average altitude, altitude standard deviation, and description of the waypoint pattern used. Each flight is plotted individually in **Figures 3.1-3.5, a,b,c,d,e** and as a combined overlay plot in **Figures 3.1-3.5, f**).

Table 3.1. Flight data from autonomous sampling flights.

				Colonies	Samplers Open Statistics		
Flight #	Date	Flying Time of Day	Media	Total	Average Altitude (m)	Altitude StDev (m)	.fly pattern
Flight1	8/13/2006		FSM	83	100*	*	rectangle
Flight2	9/11/2006		FSM	Contam	91.3	13.6	rectangle
Flight3	9/16/2006	1:15 PM	FSM	38	98.6	6.6	rectangle
Flight4	9/16/2006	3:00 PM	FSM	34	98.6	9.8	rectangle
Flight5	9/16/2006	4:30 PM	FSM	19	96.8	8.5	rectangle
Flight6	9/29/2006	6:35 PM	FSM	18	99.7	5.5	rectangle
Flight7	9/30/2006	11:10 AM	FSM	4	99.8	5.4	rectangle
Flight8	9/30/2006	11:50 AM	FSM	28	99.0	4.4	rectangle
Flight9	10/4/2006	6:35 PM	1/4 PDA	DNA	99.5	4.6	rectangle
Flight10	10/4/2006	7:00 PM	FSM	0	98.7	5.5	rectangle
Flight11	10/5/2006	4:45 PM	1/4 PDA	DNA	100.2	3.8	rectangle
Flight12	10/8/2006	10:45 AM	FSM	1	113.0	43.3	rectangle
Flight13	10/8/2006	11:30 AM	FSM	9	99.3	4.8	rectangle
Flight14	10/9/2006	4:35 PM	FSM	8	99.5	6.1	rectangle
Flight15	10/9/2006	5:15 PM	FSM	5	99.6	5.6	rectangle
Flight16	10/9/2006	6:00 PM	FSM	10	98.8	8.0	rectangle
Flight17	10/11/2006	6:20 PM	FSM	13	99.5	5.9	rectangle
Flight18	10/21/2006	11:10 AM	1/4 PDA	DNA	98.8	6.0	rectangle
Flight19	10/21/2006	12:00 PM	FSM	3	97.9	7.5	rectangle
Flight20	10/21/2006	12:50 PM	1/4 PDA	DNA	97.5	8.0	rectangle
Flight21	10/21/2006	1:35 PM	1/4 PDA	DNA	99.4	7.2	rectangle
Flight22	10/21/2006	2:15 PM	FSM	4	99.0	7.2	rectangle
Flight23	11/5/2006	3:30 PM	1/4 PDA	DNA	99.9	1.6	rectangle
Flight24	11/6/2006	11:25 AM	FSM	3	99.9	2.4	rectangle
Flight25	11/6/2006	11:55 AM	1/4 PDA	DNA	93.0	15.8	fig8
Flight26	11/9/2006	4:00 PM	FSM	3	100.0	3.5	rectangle
Flight27	11/9/2006	4:30 PM	1/4 PDA	DNA	100.0	3.1	point
Flight28	11/10/2006	10:50 AM	FSM	5	99.9	5.7	fig8
Flight29	11/10/2006	11:25 AM	FSM	1	97.9	11.9	rectangle
Flight30	11/10/2006	11:55 AM	1/4 PDA	DNA	100.0	2.8	rectangle
Flight31	11/10/2006	4:25 PM	FSM	5	100.0	5.1	fig8
Flight32	11/10/2006	4:55 PM	FSM	8	100.3	5.0	rectangle
Flight33	11/11/2006	12:05 PM	FSM	5	99.9	3.9	fig8
Flight34	11/11/2006	1:20 PM	FSM	8	99.9	1.9	point
Flight35	11/24/2006	3:40 PM	FSM	1	99.9	1.6	point
Flight36	11/25/2006	11:45 AM	FSM	1	99.8	2.2	rectangle
Flight37	11/25/2006	12:15 PM	FSM	1	99.9	2.5	triangle
Flight38	11/25/2006	12:45 PM	FSM	0	99.9	2.5	triangle
Flight39	11/25/2006	1:30 PM	FSM	0	99.9	2.8	triangle
Flight40	11/25/2006	2:00 PM	1/4 PDA	DNA	60.0	1.8	point
Flight41	11/25/2006	2:30 PM	1/4 PDA	DNA	199.9	2.0	point
Flight42	11/25/2006	3:00 PM	FSM	0	299.9	2.8	point
Flight43	11/25/2006	3:30 PM	FSM	1	100.0	6.1	line
Flight44	12/18/2006	1:00 PM	FSM	4	100.0	4.7	rectangle
Flight45	1/15/2007	12:40 PM	FSM	0	62.3	4.9	point_RC
Flight46	2/1/2007	5:15 PM	1/4 PDA	DNA	100.0	1.6	rectangle
Flight47	2/17/2007	4:00 PM	1/4 PDA	DNA	100*	*	line
Flight48	2/24/2007	11:45 AM	1/4 PDA	DNA	100.0	7.26	line
Flight49	2/24/2007	12:45 PM	FSM	0	99.9	2.49	rectangle
Flight50	2/24/2007	1:30 PM	1/4 PDA	DNA	99.9	3.96	line
Flight51	2/24/2007	2:10 PM	1/4 PDA	DNA	95.2	14.42	line
Flight52	2/24/2007	3:20 PM	1/4 PDA	DNA	100.0	4.72	line
Flight53	2/24/2007	3:45 PM	FSM	1	99.8	3.20	rectangle
Flight54	2/28/2007	9:45 AM	FSM	0	99.9	5.36	fig8
Flight55	2/28/2007	10:15 AM	1/4 PDA	DNA	99.9	4.91	fig8
Flight56	2/28/2007	10:50 AM	1/4 PDA	DNA	99.9	3.84	fig8
Flight57	3/15/2007	3:00 PM	FSM	0	100.0	6.85	fig8
Flight58	3/25/2007	10:30 AM	1/4 PDA	DNA	100.0	3.45	triangle
Flight59	3/25/2007	11:30 AM	FSM	4	100.0	4.99	triangle
Flight60	4/24/2007	7:45 PM	FSM	2	100*	*	point
Flight61	4/30/2007	10:15 AM	FSM	2	100.0	9.20	point
Flight62	4/30/2007	11:00 AM	FSM	1	99.9	9.67	point
Flight63	5/1/2007	10:00 AM	FSM	36	99.9	2.49	point
Flight64	5/1/2007	11:00 AM	FSM	21	99.9	4.54	point
Flight65	5/1/2007	4:15 PM	FSM		99.9	9.37	point
Flight66	5/1/2007	6:00 PM	FSM	3	99.7	8.22	point
Flight67	5/2/2007	10:00 AM	FSM		99.9	3.57	point

* datalog was not downloaded due to internal error of the autopilot

The single waypoint pattern exhibited no unpredicted behavior in any of the flights. The altitude hold of this pattern resulted in standard deviations ranging from 1.6 to 2.8 meters. GPS noise, shown by sharp changes in path direction, created an artificial inconsistency in the sampling pattern. This noise may be explained by fluctuations in weather conditions, interference, or the position of tracked satellites.

The two GPS waypoint pattern showed some unreliability in the way that the plane reversed direction from clockwise to counter-clockwise during flight. Reversing direction during flight changed the angle at which the plane approached each waypoint and therefore introduced a large positional inconsistency. This pattern also didn't hold as tight a tolerance on altitude because the plane had to make a hard bank at both ends of the pattern. The three GPS waypoint pattern did fairly well on positional accuracy, but did not maintain altitude for the same reasons as the two point pattern. The four GPS waypoint pattern showed good positional accuracy and very good accuracy in maintaining altitude with standard deviations ranging from 1.6 to 4.7 meters. The figure-8 pattern did not have high positional accuracy, but appeared better than the two GPS waypoint pattern. It was also not a strong performer in altitude hold due to the sharp turns on both ends of the patterns.

Our UAV is capable of maintaining a very precise altitude for the duration of a sampling flight (**Figure 3.7**). A range of ±5 meters around the target altitude was obtained during many flights with standard deviations less than two meters. The RC flight used as a comparison shows the differences between RC flight and autopilot flight. The flight data is represented by Flight 45 (**Table 3.1 and Figure 3.6**). The standard deviation for the RC flight was more than twice that of the autonomous flight for the

same flight pattern. This pattern was chosen since it appeared to be the best autonomous pattern and was also the easiest to fly in RC mode. The pattern was easiest since the flight path was a constant turn and it never required the UAV to be very far from the pilot making it more controllable. From that point of view, it can be assumed that trying to fly the other patterns RC would only result in limited positional accuracy and altitude hold.

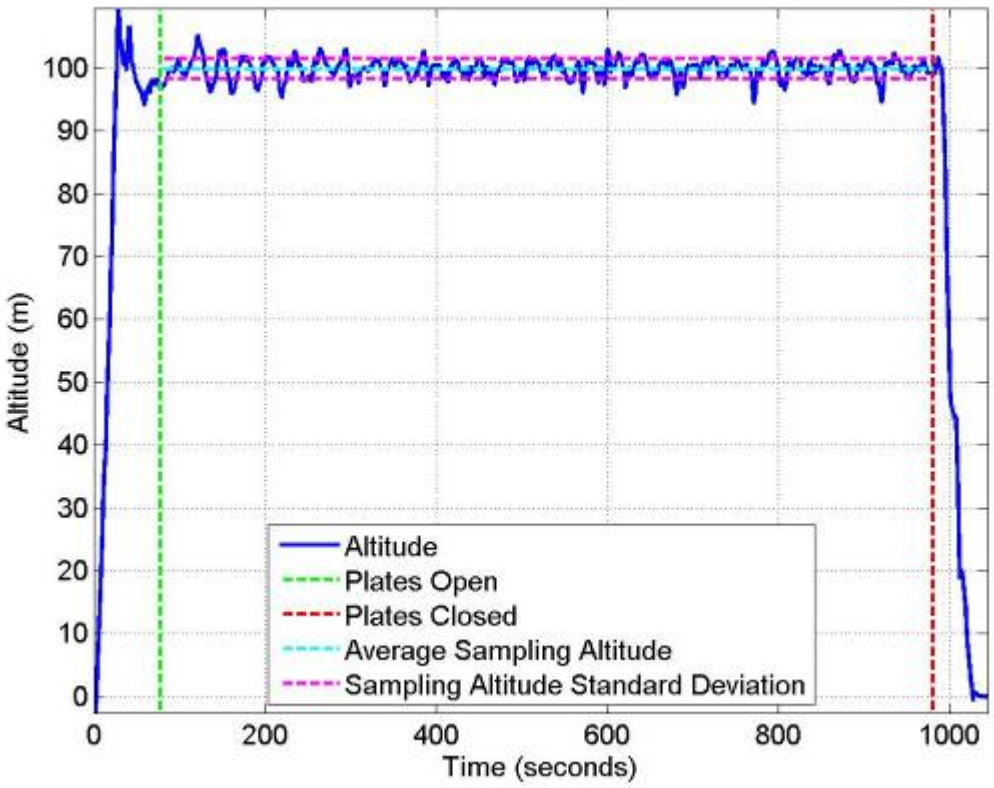

Figure 3.7. Maintenance of a precise altitude during aerobiological sampling.

All of the GPS waypoint patterns performed well in holding altitude accuracy relative to the accuracy of a standard RC RPV as used in the past (Shields, 2006). Two of the patterns stand out as the most consistent sampling paths within flights and across different flights. These two patterns are the single point pattern (**Figure 3.1**) and the four point rectangular pattern (**Figure 3.4**). Both these patterns have very good positional

accuracy and an altitude range of ±5 meters around the target altitude with standard deviations less than two meters on many flights. Both of these patterns are practical for aerobiological sampling in agricultural fields.

CHAPTER 4

EXTENDED WORK WITH NEW AND ALTERNATIVE AUTONOMOUS UNMANNED AERIAL VEHICLE SYSTEMS

THE SIG RASCAL 110" AS A NEW AEROBIOLOGICAL SAMPLING PLATFORM

Platform.

The Rascal 110" (SIG Manufacturing Co., Inc., Montezuma, IA) was chosen as an alternative UAV platform to the Senior Telemaster due to its larger size and higher payload capabilities (**Figure 4.1**). It was also a good choice since other collaborating groups are also using this platform and therefore parts could be borrowed or interchanged as needed.

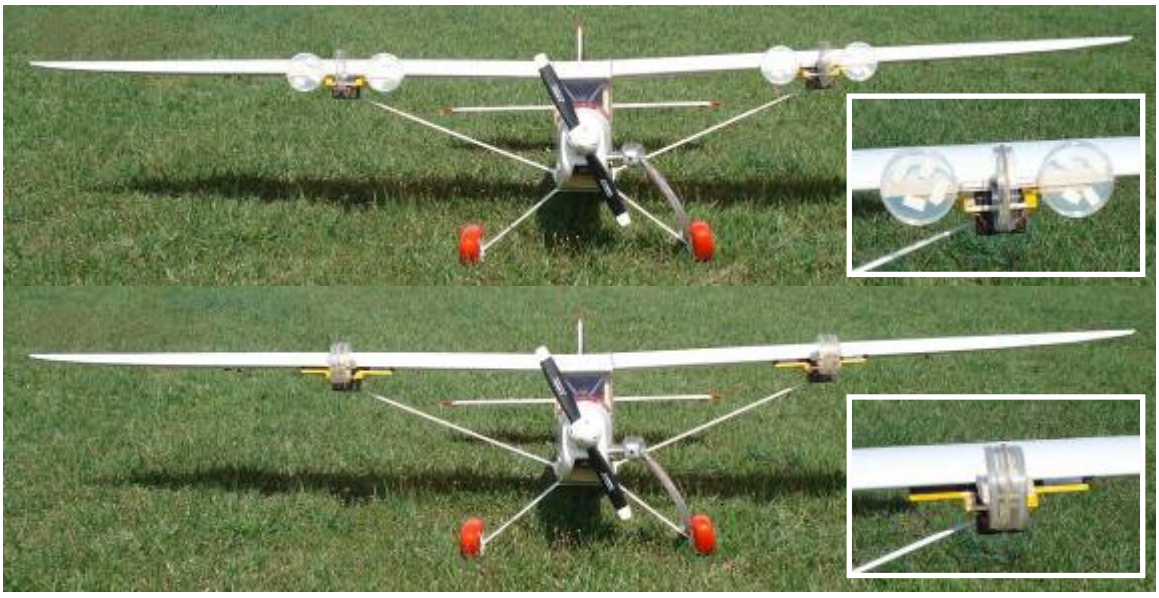

Figure 4.1. Rascal 110" as a shown with samplers open (a) and samplers closed (b).

The Rascal 110" was built to accommodate two different engines. The first engine used was O.S. 1.20 in^3 (O.S. Engines), the same engine used on the Telemaster.

This engine was in the recommended size range for this aircraft but still performs very well with the extra payload and drag of the spore-sampling devices. The second engine used is the O.S. 1.60 in^3 (O.S. Engines) which has 3.7 hp and is turning a 18x10 inch Classic Series Master Airscrew propeller (Windsor Propeller Company). The larger engine is more powerful but consumes a great deal more fuel. This engine can consume 24 oz of fuel in less than 14 minutes at full throttle. The factory 15 oz fuel tank was replaced with a 24 oz fuel tank to allow for longer flight times. To accommodate this larger tank, the factory tank mount had to be `h and custom firewall mounts installed on which the tank could rest. It was desirable to move the servos out of the normal mounting locations in the center of the UAV to free up more space for other components and wiring. The throttle servo was moved forward and mounted on a custom bracket (**Figure 4.2**). The factory throttle servo pushrod, which was a plastic tube-in-tube type, was replaced with a solid metal pushrod to make the throttle response more precise. The pull-pull rudder servo was not installed, but instead a standard pushrod and servo was installed near the tail to actuate the rudder. This eliminated the servo wires of the pull-pull design that normally ran the entire length of the fuselage. There is a factory cut slot in the tail to allow the movement of the rudder servo. The window on the opposite side of the muffler was replaced with a custom plywood camera mount. This enabled the UAV to carry a digital camera to record video or to take high resolution digital images of the fields below.

Figure 4.2. Relocated throttle servo to create space for autonomous unit and ensure consistent throttle response.

Electronics box. The same basic approach as used on the Telemaster was used to incorporate the electronic components into the UAV. A standard project box was modified to house the autopilot, compass, GPS receiver, and servo board (**Figure 4.3**). Holes were cut in the front of the box to mount the GPS antenna cable and the autopilot communications port. On the back of the box, holes were cut to mount two power connection cables and a larger hole was cut for the servo board to allow the servo signal wires to be plugged into the appropriate terminals. The pitot tube was also routed through the back of the box via a 90º vacuum elbow.

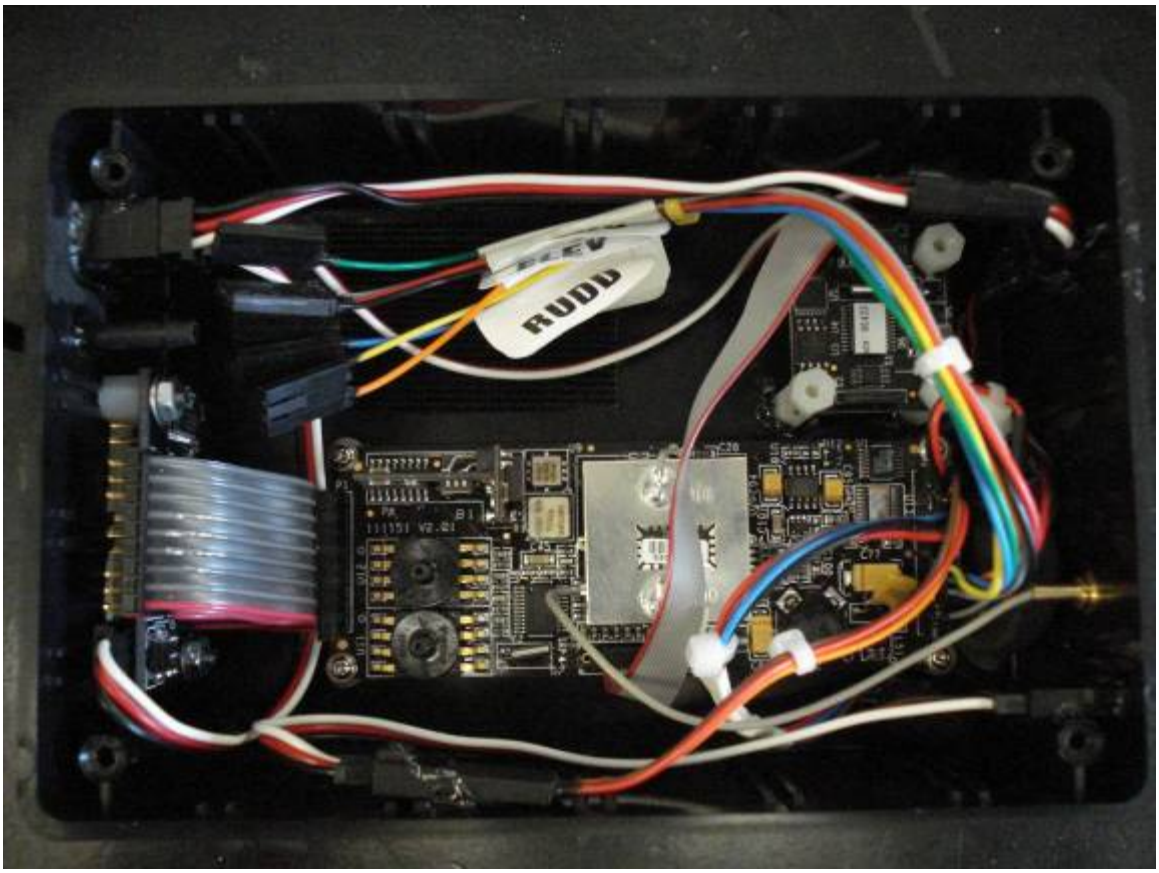

Figure 4.3. Electronics box for Rascal 110".

Redundant control via the RxMUX. An additional safety feature was added to the Rascal UAV that increases safety for humans and for the expensive equipment onboard the UAV. The RxMUX (Reactive Technologies, Merrimack, NH) allows the addition of a second RC receiver to be added to the UAV for redundant control from the ground. The RxMUX is a signal multiplexer that takes inputs from two RC receivers and outputs one signal to control the servos of the UAV (**Figure 4.4**) (Dingus et al, 2007). In this case, the primary source of control is the autopilot, which can be controlled by its own RC receiver. The secondary source of control is the backup RC receiver on a different channel from the autopilot. The receiver that passes through the autopilot has a channel that allows the safety pilot to reclaim control at any time with the flip of a switch on the

transmitter. The RxMUX also allows one channel of the input to control which input source is controlling the servos. With this setup, the UAV can be operated independently with either transmitter. In other words, only one of the two transmitters is needed to fly the UAV at any given time. If only the autopilot transmitter is used, the pilot is able to pass control back and forth to the autopilot. If only the backup transmitter is used, the UAV can only be flown in RC controlled mode. But with the combination of the two, two pilots can be watching the UAV during flight where both have the ability to take control from the autopilot if something goes wrong. If the secondary transmitter takes control of the UAV, then the primary transmitter and the autopilot can not take control back at any time. The secondary backup pilot has to give control back the primary transmitter or autopilot. This system allows the pilot to be in two different locations with two different views of the UAV and whoever has the best view of the UAV can have control. The only time that communication between the two pilots is needed is when the secondary backup transmitter gives control back the primary transmitter.

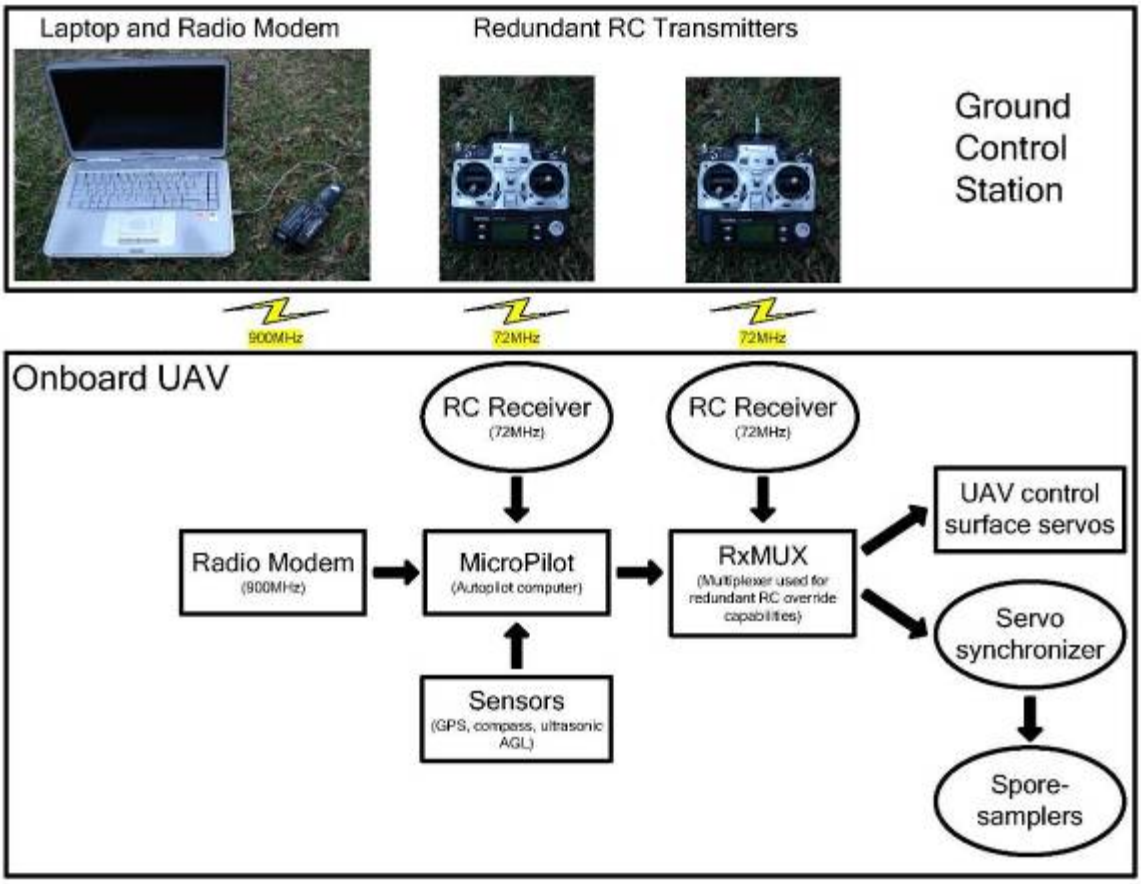

Figure 4.4. The RxMUX allows for redundant RC control from the ground for safety.

SPORE-SAMPLERS

The same spore samplers that were described for the Senior Telemaster were used on the Rascal. The samplers could be interchanged between UAVs freely since they are made exactly the same way. A newly designed sampler was created to allow for more flexible data collection. The new design uses smaller 60 mm petri plates with a total of six per sampler (**Figure 4.5**). The only modifications the old sampler design were changing the arm the plates attached to and the piece of plywood in the center of the samplers that the plates close onto. Each arm was created to hold three plates in a straight line. With this

design, multiple media types can be used in one flight. This allows comparison of different samples taken at exactly the same time.

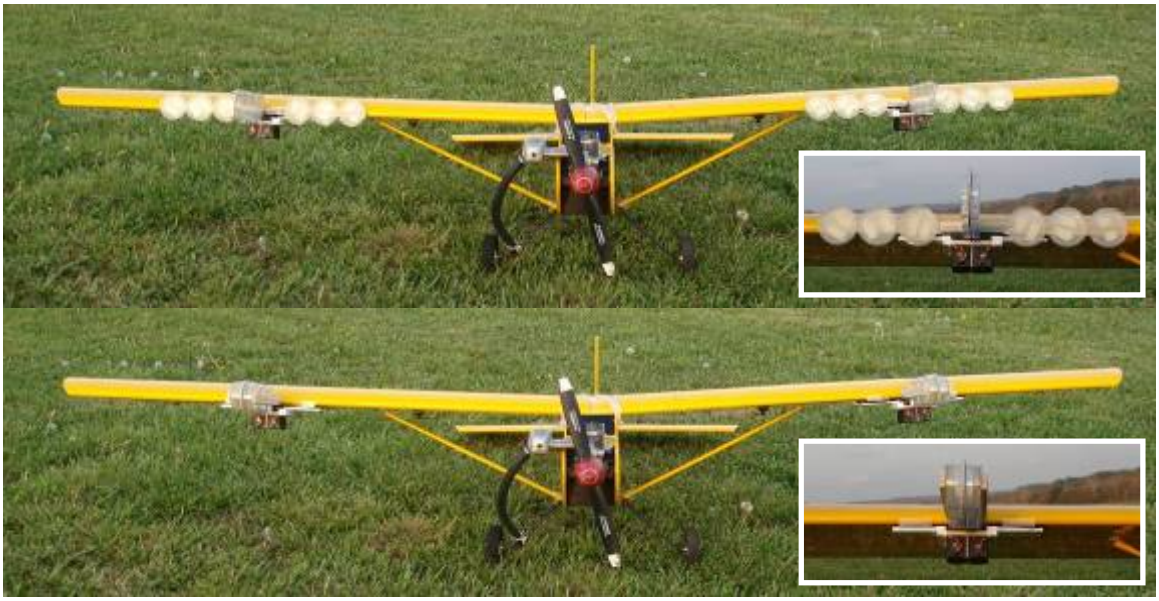

Figure 4.5. Redesigned sampling devices allow for greater flexibility of media used.

CHAPTER 5

CONTRIBUTIONS, RECOMMENDATIONS, AND FUTURE WORK

CONTRIBUTIONS

We believe that our work using UAVs for aerobiological sampling has resulted in several research milestones. We completed the first autonomous sampling flight. We believe this has produced the most consistent aerobiological sampling path recorded and the most consistent aerobiological sampling height. We also completed the first autonomous sampling using 12 individual sampling plates in one sampling flight. We also believe our sampling has resulted in the first examination of entire *Fusarium* populations in the atmosphere, 100 m above the ground. Previous work was only concerned with a single *Fusarium* species, Gibberella zeae (Maldonado-Ramirez et al., 2005). We also are the first to examine entire atmospheric microbial communities.

RECOMMENDATIONS

Coordinated sampling with the Piccolo autonomous system. A recommendation to further extend the capabilities of our UAVs is to use the Piccolo (Cloud Cap Technology, Hood River, OR) family of autopilots. With Piccolo autopilots the UAVs could relatively easily be programmed to fly coordinated flight paths. This is an extension of the simultaneous flights mentioned previously where the plane are just in the air at the same time flying the same predefined waypoints. With Piccolo, a small amount of user written-code could make one UAV a master and any number of other UAVs slaves following the commands of the master resulting in UAVs not only flying the same path

but flying the same path at same positional location at the same time to result in truly coordinated flight. The concept of this coordinated vehicle communication has already been proven at Virginia Tech by coordination of an unmanned ground vehicle (UGV) and a UAV where the UGV was the master and the UAV was the slave monitoring the UGV from above.

FUTURE WORK

Night-time flight. There are a few additional objective planned for our UAVs to make them even more functional. We will add navigation lights to enable flights at night. The most appealing light source that we have located is the RC Airplane Beacon (Rod-N-Bobb's, Eau Claire, WI) which is a complete lightweight unit that provides red, green, and yellow lights for the left wing, right wing, and tail, respectively. Many interesting questions can be answered with nighttime flights. With this capability, we will be able to sample the atmosphere at anytime during the day or night. For example, we could sample for a 24 hour period every hour. To our knowledge, this has never been done before. Since the system is autonomous, the only part of the flight that he pilot has to do is the takeoff and landing which makes the RC pilot's tasks far less stressful.

Simultaneous UAVs for aerobiological sampling at multiple altitudes. As soon as the Racal 110" platform is fully developed and navigating precisely, we will use two or more UAVs in the air at one time at different altitudes. This will require multiple pilots preparing multiple planes on the ground. We will takeoff one plane and climb to the higher of the desired altitudes. The second plane will then takeoff and climb to the lower

of the desired altitudes. At that time, we will set both planes into in autonomous mode where they will enter the desired flight path. This can also answer some interesting questions having two precisely controlled UAVs navigating the atmosphere collecting samples at different altitudes at exactly the same time.

LITERATURE CITED

Dingus, B., Hoppe, L., Lee, J., Misyak, N., Pape, D., Ryan, J., Schivikas, M., Shake, S., Veraa, C., and Reinholtz, C. 2006. Development of a fixed-wing autonomous aerial vehicle at Virginia Tech.

Dingus, B., Schmale, D.G., Reinholtz, C.F., 2007. Development of an autonomous unmanned aerial vehicle (UAV) for aerobiological sampling. APS Potomac Division Meeting.

Flight Global, MicroPilot unveils own agricultural UAV to help shape civil market evolution. November 2006. Online. Internet. April 2007. <http://www.flightglobal.com/articles/2006/09/11/208933/micropilot-unveils-own-agricultural-uav-to-help-shape-civil-market.html>

Maldonado-Ramirez, S.L., Schmale, D.G., Shields, E.J., and Bergstrom, G.C. 2005. The relative abundance of viable spores of *Gibberella zeae* in the planetary boundary layer suggests the role of long- distance transport in regional epidemics of Fusarium head blight. Agric. For. Meteorol. 132: 20-27.

Ramirez, Rachael A., 2006. Computer Vision Based Analysis of Broccoli for Application in a Selective Autonomous Harvester.

Shields, E.J., Testa, A.M., 1999. Fall migratory flight initiation of the potato leafhopper, Empoasca fabae (Homoptera: Cicadellidae): observations in the lower atmosphere using remote piloted vehicles. Agric. Forest Meteorol. 97, 317–330.

Shields, E. J., J. T. Dauer, M. J. Van Gessel, and G. Neumann. 2006. Horseweed (*Conyza Canadensis*) seeds collected in the planetary boundary layer. Weed Sci. 54:1063-1067.